

Interaction of Pyridine-2,6-dicarboxylic Acid with Cr(VI) in the Oxidative Decarboxylation of Phenylsulfinyl Acetic Acid and Linear Free Energy Relationship

Perumal Subramaniam^{1*} and Natesan Thamil Selvi²

¹Research Department of Chemistry, Aditanar College of Arts and Science, Tiruchendur-628 216, Manonmaniam Sundaranar University, Tamil Nadu, India.

²Department of Chemistry, Govindammal Aditanar College for Women, Tiruchendur-628 215, Manonmaniam Sundaranar University, Tamil Nadu, India.

Authors' contributions

This work was carried out in collaboration between both authors. Author NTS designed the study, performed the statistical analysis, wrote the protocol, and wrote the first draft of the manuscript. Authors PS and NTS managed the analyses of the study. Author NTS managed the literature searches. Both authors read and approved the final manuscript.

Article Information

DOI: 10.9734/ACSj/2015/15998

Editor(s):

(1) Nagatoshi Nishiwaki, Kochi University of Technology, Japan.

Reviewers:

(1) Anonymous, Poland.

(2) Anonymous, Morocco.

Complete Peer review History: <http://www.sciencedomain.org/review-history.php?id=900&id=16&aid=8182>

Original Research Article

Received 31st December 2014

Accepted 22nd January 2015

Published 20th February 2015

ABSTRACT

Aims: To investigate the catalytic activity of pyridine-2,6-dicarboxylic acid in the redox reaction of Cr(VI) and phenylsulfinyl acetic acid.

Study Design: The mechanism of the reaction was designed on the basis of the observed results of kinetic, spectral and substituent effect studies.

Place and Duration of Study: Laboratory of the Research Department of Chemistry, Aditanar College of Arts and Science, Tiruchendur, Tamil Nadu, India. September 2013 – January 2014.

Methodology: Phenylsulfinyl acetic acid and ten *meta*- and *para*-substituted phenylsulfinyl acetic acids essential for the present kinetic study were synthesized. The kinetic study was performed in 40% acetonitrile-60% H₂O medium under pseudo-first-order conditions by maintaining [PSAA] >>

*Corresponding author: E-mail: subramaniam.perumal@gmail.com;

[Cr(VI)] throughout the experiment. The progress of the reaction was monitored by following the rate of disappearance of Cr(VI) spectrophotometrically at 351 nm. The effect of pyridine-2,6-dicarboxylic acid on the rate of the reaction and the applicability of linear free energy relationship with different phenylsulfinyl acetic acids were tested.

Results: The reaction shows unit order dependence on Cr(VI) but follows Michaelis-Menten kinetics with respect to substrate as well as catalyst. The order with respect to $[H^+]$ is between one and two. The thermodynamic parameters $\Delta^\ddagger S$ ($-93.2 \text{ JK}^{-1} \text{ mol}^{-1}$) and $\Delta^\ddagger H$ (57.7 kJ mol^{-1}) are evaluated respectively from the intercept and slope of the Eyring's plot. The Hammett's correlation affords a negative ρ value (-1.05).

Conclusion: Pyridine-2,6-dicarboxylic acid catalyzes the reaction and Cr(VI)-PDA complex is assumed to be the oxidizing species of the reaction. The sulfur of PSAA undergoes nucleophilic attack on Cr(VI)-PDA complex forming a ternary complex, Cr(VI)-PDA-PSAA which experiences decarboxylation, ligand coupling and further decomposition giving methylphenyl sulfone as the product. The mechanism with the associated reaction kinetics is assigned in support of substituent effect.

Keywords: Phenylsulfinyl acetic acid; pyridine-2,6-dicarboxylic acid; catalytic activity; Michaelis-Menten kinetics; substituent effect.

1. INTRODUCTION

Pyridine-carboxylic acids occupy prime importance in research as they are excellent ligands [1] and good synthons for supramolecular architectures and coordination polymers [2]. These ligands have structural adaptability to self-assemble into two or three dimensional frameworks either using hydrogen bonding or by polymerization. Pyridine mono- and di- carboxylic acids are prominent ligands from catalytic and crystal engineering point of view. Pyridine-2,6-dicarboxylic acid (PDA) is found to be a versatile N, O chelator due to its diverse coordination modes [1,3,4]. It forms stable chelates with various metal ions and its chelates with some transition metals have beneficial effects in normalizing elevated blood glucose levels [5,6]. PDA enhances the Fenton reaction in phosphate buffer and it is an antiseptic [7]. PDA is reported as an efficient eluent in the chromatographic separation of transition metals and is also used for the quantitative determination of several metals [8]. Derivatives of PDA are ubiquitous in biology and medicine for analytical and diagnostic purposes [9-12] due to their strong fluorescence intensity with relatively long excitation lifetimes. These luminescent complexes can act as efficient light-conversion molecular devices (LCMD). It is also reported that PDA is used to develop more effective anti HIV agents [13].

The report on the utility of such a versatile ligand as a catalyst in the Cr(VI) oxidation of organic substrates is limited. Phenylsulfinyl acetic acid (PSAA), a pharmaceutically important compound

also finds extensive application in the synthetic field. From literature survey it is apparent that no systematic work has been reported so far on the oxidation kinetics of PSAA except our recent reports [14-17]. Hence, this study was performed to acquire more information on the role of PDA in the reduction of Cr(VI) by PSAA, the oxidizing species involved in the reaction and the plausible mechanism of the reaction based on kinetic and spectral evidences.

2. EXPERIMENTAL DETAILS

2.1 Materials

The substrates, PSAA and several *meta*- and *para*-substituted PSAAs essential for the present kinetic study were synthesized [18] by the controlled oxidation of the corresponding phenylthio acetic acids using equimolar amount of H_2O_2 . Then the samples were recrystallized from suitable solvents and stored in vacuum desiccator. Their melting points were determined and compared with the literature values [19]. The purity was also checked by LCMS. Potassium dichromate (Merck), sodium perchlorate (Merck), $HClO_4$ (Merck) and pyridine-2,6-dicarboxylic acid (SDs) were of AnalaR grade and the stock solutions were prepared using double distilled water. The solvent, acetonitrile was used after purification by literature method [20].

2.2 Kinetic Measurements

The reaction mixture, under the conditions $[PSAA] \gg [Cr(VI)]$ and $[PDA] \gg [Cr(VI)]$ was

used for the kinetic runs throughout the experiment. Progress of the reaction was monitored by following the rate of disappearance of Cr(VI). The reaction mixture was scanned in the range 200-700 nm using UV-vis spectrophotometer at regular intervals to follow the gradual development of intermediate if any and product. The spectral changes associated with the PDA catalyzed oxidative decarboxylation of PSAA are shown in (Fig. 1).

The pseudo-first-order rate constant (k_1) for each kinetic run was evaluated from the slope of log OD vs. time by the method of least squares. The overall rate constant of the PDA catalyzed reaction is calculated using the eq. (1),

$$k_{ov} = \frac{k_1}{[PSAA]^n} \quad (1)$$

where n is the order of the reaction with respect to PSAA and k_1 is the observed pseudo-first-order rate constant for the PDA catalyzed reaction. The precision of the k values is given in terms of 95% confidence limits of student's t test.

2.3 Product Analysis

The reaction mixture in the stoichiometric condition was kept for 48 hours to ensure completion of the reaction. The solvent was then evaporated and extracted with ether. The ether layer was collected, dried over anhydrous sodium sulfate and the ether was removed by evaporation. IR and GC-MS analysis of the residue obtained from the ether extract confirm that methylphenyl sulfone is the only product of the reaction. IR spectrum shows strong bands at 1148 cm^{-1} and 1290 cm^{-1} characteristic of symmetric and asymmetric stretching respectively of $>\text{SO}_2$ group [21].

The absorption spectra of the reaction mixture after completion exhibits two distinct peaks: one at 577 nm and another at 434 nm corresponding to ${}^4\text{A}_{2g}(\text{F}) \rightarrow {}^4\text{T}_{2g}(\text{F})$ and ${}^4\text{A}_{2g}(\text{F}) \rightarrow {}^4\text{T}_{1g}(\text{F})$ transitions respectively of the Cr(III) species [22,23]. Comparison of this spectrum with that of the authentic Cr(III) sample and the spectrum of the product mixture in the uncatalyzed reaction [15] clearly shows a blue shift which supports the existence of Cr(III) in the form of complex probably with PDA as evidenced by several researchers [24-27] with different catalysts. This is further confirmed from the colour of the

product mixture which is purple in colour instead of the characteristic green colour of Cr(III).

3. RESULTS AND DISCUSSION

The linear rate of disappearance of Cr(VI) shows first-order dependence on $[\text{Cr(VI)}]$ and the pseudo-first-order rate constants evaluated from the linear plots of log OD vs. time are given in (Table 1). The rate data show that the pseudo-first-order rate constant is found to decrease appreciably with increase in $[\text{Cr(VI)}]$. Similar type of rate retardation has been reported in the EDTA catalyzed Cr(VI) oxidation of phenylmercaptoacetic acid [28] and PA catalyzed Cr(VI) oxidation of DMSO [29]. This may be rationalized as dimerization of Cr(VI) oxidizing species at higher concentrations followed by decrease in concentration of active species.

The pseudo-first-order rate constants calculated for the variation of $[PSAA]$ in the presence of PDA show a linear increase with increase in concentration of PSAA (Table 1). The non-constancy of k_2 values observed indicates that the order with respect to $[PSAA]$ is not unity but fractional. The Michaelis-Menten kinetics, eq.(2) with respect to PSAA for the PDA catalyzed reaction is proved from the linear ($r = 0.999$) double inverse plot of k_1 vs. $[PSAA]$ with intercept on the rate axis. The values of k and K_m evaluated from the slope and intercept of the plot are $3.24 \times 10^{-3} \text{ s}^{-1}$ and $1.19 \times 10^{-1} \text{ mol dm}^{-3}$ respectively. The order with respect to PSAA is 0.79 ± 0.03 as revealed by the slope of the linear ($r = 0.999$) log-log plot of k_1 vs. $[PSAA]$.

$$\frac{1}{k_1} = \frac{1}{k} + \frac{K_m}{k[PSAA]} \quad (2)$$

3.1 Rate Dependence on Acidity and [PDA]

The effect of $[\text{H}^+]$ on the rate of the reaction is studied by varying the concentration of HClO_4 in the reaction mixture (Table 2) and found that the rate of the reaction increases with increase in $[\text{H}^+]$. Though a negligible effect of ionic strength is observed, it is maintained as constant in all the kinetic runs using sodium perchlorate.

To monitor the effect of $[PDA]$ on the rate of the reaction, the kinetic runs were performed with varying concentrations of PDA from 0.5×10^{-2} to $40 \times 10^{-2} \text{ mol dm}^{-3}$. The rate of the reaction

increases linearly with increase in the concentration of PDA and leads to limiting value at higher concentrations of PDA (Table 2, Fig. 2). The reaction shows Michaelis-Menten kinetics with respect to [PDA] as shown from the linear plot ($r = 0.993$) of k_1^{-1} vs. $[PDA]^{-1}$ not passing

through the origin. This confirms the binding of PDA with the oxidizing species prior to the rate determining step. The Michaelis-Menten constant, K_m calculated from the slope and intercept of the above plot is found to be $5.36 \times 10^{-2} \text{ mol dm}^{-3}$.

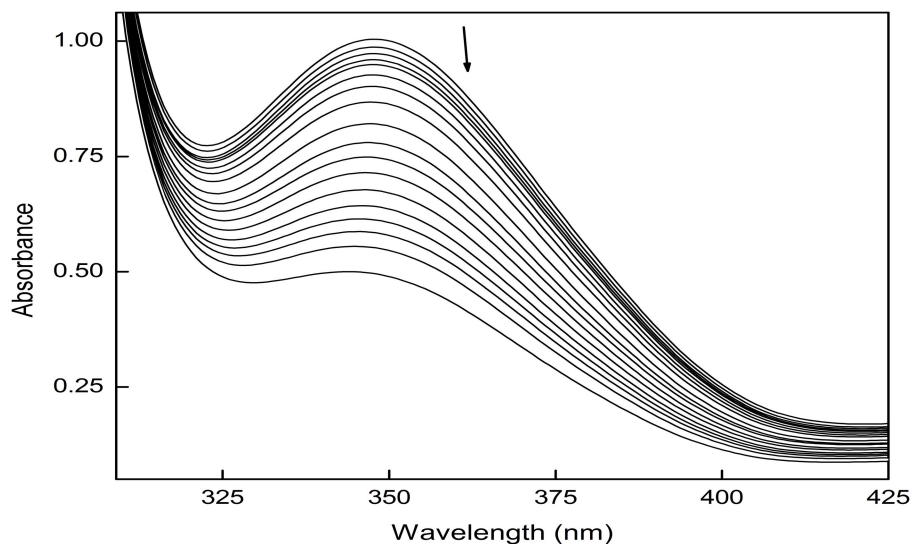


Fig. 1. UV-visible spectra of the reaction mixture in the presence of PDA
 $[PSAA] = 5.0 \times 10^{-2} \text{ mol dm}^{-3}$; $[Cr(VI)] = 5.0 \times 10^{-4} \text{ mol dm}^{-3}$; $[H^+] = 7.5 \times 10^{-1} \text{ mol dm}^{-3}$;
 $[PDA] = 5.0 \times 10^{-2} \text{ mol dm}^{-3}$; solvent = 40 % CH_3CN -60% H_2O

Table 1. Rate dependence of reactants for PDA promoted reaction at 30 °C

$10^2 [PSAA] (\text{mol dm}^{-3})$	$10^4 [Cr(VI)] (\text{mol dm}^{-3})$	$10^4 k_1 (\text{s}^{-1})$	$10^2 k_2 (\text{dm}^3 \text{mol}^{-1} \text{s}^{-1})$
1.0	5.0	2.51±0.02	2.51±0.02
3.0	5.0	6.51±0.11	2.17±0.04
5.0	5.0	9.09±0.42	1.82±0.08
7.0	5.0	12.2±0.46	1.74±0.06
10	5.0	15.6±0.56	1.56±0.06
5.0	3.0	15.8±0.22	3.16±0.04
5.0	7.0	8.17±0.14	1.63±0.03

$[PDA] = 5.0 \times 10^{-2} \text{ mol dm}^{-3}$; $[H^+] = 7.5 \times 10^{-1} \text{ mol dm}^{-3}$; $I = 8.0 \times 10^{-1} \text{ mol dm}^{-3}$;
 solvent = 40% CH_3CN -60 % H_2O

Table 2. Effect of H^+ , [PDA] and temperature on the pseudo-first-order rate constant

$[H^+] (\text{mol dm}^{-3})$	$10^4 k_1^a (\text{s}^{-1})$	$10^2 [PDA] (\text{mol dm}^{-3})$	$10^4 k_1^b (\text{s}^{-1})$	Temperature (°C)	$10^3 k_{\text{ov}}^c ((\text{dm}^3 \text{mol}^{-1})^n \text{s}^{-1})$
0.3	2.73±0.18	0	6.49±0.25	20	4.31±0.03
0.5	5.51±0.21	0.5	6.91±0.04	25	7.16±0.08
0.75	9.21±0.19	0.9	7.22±0.12	30	9.69±0.45
0.9	14.4±0.20	1.5	7.64±0.11	35	14.8±0.19
1.0	18.1±0.27	3.0	8.49±0.05	$\Delta^\ddagger H (\text{kJ mol}^{-1})$	57.7±1.94
		5.0	9.09±0.42	$-\Delta^\ddagger S (\text{JK}^{-1} \text{mol}^{-1})$	93.2±6.77
		7.0	10.3±0.12		
		8.0	11.7±0.07		
		15	14.3±0.05		
		30	15.9±0.11		
		40	16.2±0.09		

$[Cr(VI)] = 5 \times 10^{-4} \text{ mol dm}^{-3}$; $[PSAA] = 5 \times 10^{-2} \text{ mol dm}^{-3}$; $I = 1.1 \text{ mol dm}^{-3}$; $b, c] = 8.0 \times 10^{-1} \text{ mol dm}^{-3}$; $b, c [H^+] = 7.5 \times 10^{-1} \text{ mol dm}^{-3}$;
 $a, c [PDA] = 5 \times 10^{-2} \text{ mol dm}^{-3}$; solvent = 40% CH_3CN -60% H_2O ; a, b Temp. = 30°C; n = order w.r.t. PSAA

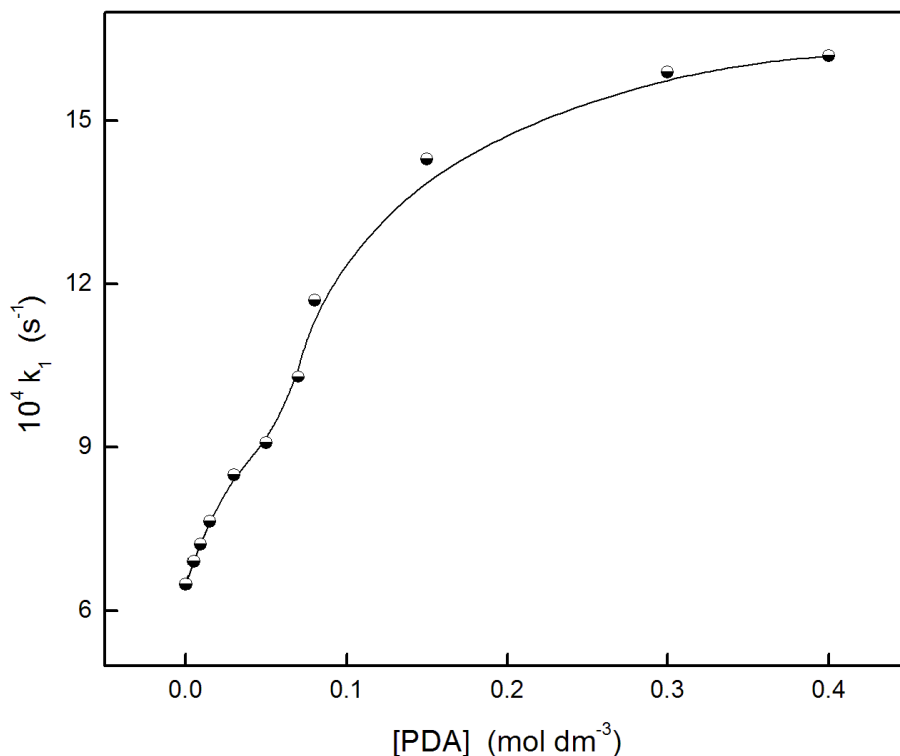


Fig. 2. Effect of [PDA] on the reaction rate
 $[PSAA] = 5 \times 10^{-2} \text{ mol dm}^{-3}$; $[Cr(VI)] = 5 \times 10^{-4} \text{ mol dm}^{-3}$; $[H^+] = 7.5 \times 10^{-1} \text{ mol dm}^{-3}$;
 $I = 8.0 \times 10^{-1} \text{ mol dm}^{-3}$; solvent = 40% CH_3CN -60% H_2O

3.2 Effect of Temperature

In order to calculate the activation parameters for the PDA catalyzed reaction, the reaction is carried out at four different temperatures viz., 20, 25, 30 and 35°C and the overall rate constant values are presented in (Table 2). The thermodynamic parameters $\Delta^\ddagger S$ and $\Delta^\ddagger H$ are evaluated respectively from the intercept and slope of the Eyring's plot of $\log k_{ov}/T$ vs. $1/T$. It is worthwhile to mention here that the observed magnitude of entropy of activation for the PDA promoted reaction is appreciably higher than that calculated for the uncatalyzed reaction [15] ($\Delta^\ddagger S = -24.5 \text{ JK}^{-1} \text{ mol}^{-1}$) which follow the trend expected for the catalyzed reactions.

3.3 Linear Free Energy Relationship

The Hammett equation and its modified forms, all known as linear free energy relationships (LFER) have been found useful for correlating the reaction rates of *meta*- and *para*-substituted derivatives. A systematic study of LFER is made on PDA catalyzed oxidative decarboxylation with several *para*- and *meta*-substituted PSAA's at

30°C to establish the effect of substituents on reactivity, to decide the nature of the transition state and the mechanism being followed. The introduction of electron-donating substituents in the *para*- and *meta*-positions of the phenyl ring of PSAA accelerates the rate appreciably while electron-withdrawing substituents decelerate the rate and the pseudo-first-order and the overall rate constants obtained are summarized in (Table 3). The Hammett plot (Fig. 3) examines the redox activity of Cr(VI) towards several substituents in the *meta*- and *para*- positions of the phenyl ring of PSAA and addresses the feasibility of the PDA catalyzed reaction with respect to them. Excellent correlation is obtained when $\log k_{ov}$ are plotted against Hammett substituent constants, σ with negative reaction constant, ρ . The negative ρ value clearly demonstrates the involvement of electron deficient reaction center in PSAA in the slow step. The linear free energy correlation corresponding to PDA catalyzed reaction is:

$$\log k_{ov} = -1.05 \pm (0.03) \sigma - 2.05$$

$$(r = 0.996; s = 0.025; n = 11) \quad (3)$$

An important point to be noted regarding the magnitude of ρ value is that the observed ρ value is smaller in the presence of PDA than in its absence [15].

Table 3. Effect of substituents on PDA catalyzed reaction at 30°C

X	PDA	
	$10^4 k_1$ (s ⁻¹)	$10^3 k_{ov}$ (dm ³ mol ⁻¹) ⁿ s ⁻¹
<i>m</i> -Br	3.36±0.01	3.58±0.01
<i>m</i> -Cl	3.38±0.04	3.60±0.04
<i>m</i> -F	3.54±0.04	3.78±0.04
<i>p</i> -Cl	4.81±0.06	5.13±0.06
<i>p</i> -Br	4.25±0.06	4.53±0.07
<i>p</i> -F	6.69±0.11	7.13±0.12
H	9.09±0.42	9.69±0.45
<i>m</i> -CH ₃	9.56±0.29	10.2±0.31
<i>p</i> -CH ₃	11.8±0.10	12.6±0.11
<i>p</i> -OC ₂ H ₅	14.5±0.08	15.5±0.09
<i>p</i> -OCH ₃	16.1±0.08	17.2±0.09
ρ	-1.05±0.03	
<i>r</i>	0.996	

$[X-C_6H_4SOCH_2COOH] = 5 \times 10^{-2} \text{ mol dm}^{-3}$; $[Cr(VI)] = 5 \times 10^{-4} \text{ mol dm}^{-3}$;
 $[H^+] = 7.5 \times 10^{-1} \text{ mol dm}^{-3}$; $I = 8.0 \times 10^{-1} \text{ mol dm}^{-3}$;
 solvent = 40% CH₃CN-60% H₂O;
 $[PDA] = 5 \times 10^{-2} \text{ mol dm}^{-3}$; $n = \text{order w.r.t. PSAA}$

3.4 Mechanism

Under the present experimental conditions of high $[H^+]$ and low $[Cr(VI)]$, $HCrO_3^+$ species was proposed as the predominant form of Cr(VI) [14,15]. The increase in reaction rate with increase in concentration of H^+ with the ligand is in agreement with the existence of $HCrO_3^+$ species. In the presence of ligands it has been observed that the redox potential of Cr(VI) increases drastically [30,31] by forming complexes with them. In many ligand catalyzed reactions of Cr(VI) oxidation, the complex formed between Cr(VI) species and ligand is identified as reactive species and its oxidizing power is believed to be higher than free Cr(VI) ion.

The increase in reaction rate with increase in [PDA] in the present case may be attributed to the formation of kinetically active Cr(VI) oxidizing species, probably a bimolecular complex formed between $HCrO_3^+$ and PDA (Scheme 1, eq.5) and enhanced reduction potential of the Cr(VI)/Cr(IV) couple.

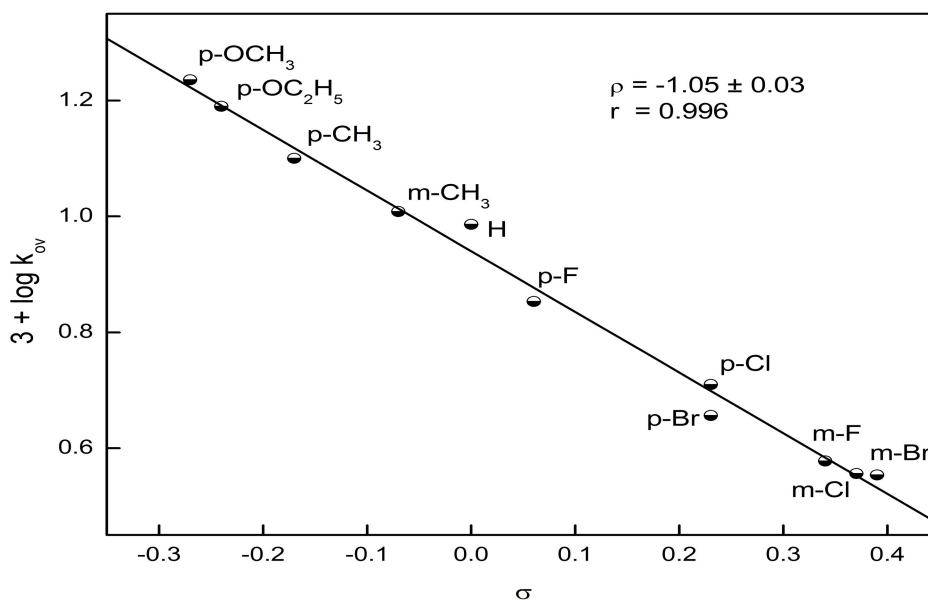


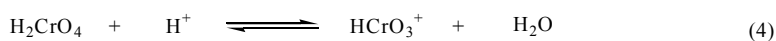
Fig. 3. Hammett plot for the PDA catalyzed reaction at 30 °C
 $[X-C_6H_4SOCH_2COOH] = 5 \times 10^{-2} \text{ mol dm}^{-3}$; $[Cr(VI)] = 5 \times 10^{-4} \text{ mol dm}^{-3}$;
 $[H^+] = 7.5 \times 10^{-1} \text{ mol dm}^{-3}$; $I = 8.0 \times 10^{-1} \text{ mol dm}^{-3}$; solvent = 40% CH₃CN-60% H₂O;
 $[PDA] = 5 \times 10^{-2} \text{ mol dm}^{-3}$

The spectral evidence for the formation of Cr(VI)-PDA complex (C_1) is inferred from the substantial hyperchromic shift and broadening of the UV absorption peak of Cr(VI) (Fig. 4a) at 263 nm by the addition of PDA (Fig. 4b). The kinetic evidence for the reversible complex formation between PDA and $HCrO_3^+$ is inferred from the Michaelis-Menten kinetics observed with PDA. The moderately low Michaelis-Menten constant value and the saturation kinetics observed with PDA (Table 2) demonstrate the existence of strong binding between $HCrO_3^+$ and PDA in the bimolecular complex, C_1 .

The chromium atom of Cr(VI)-PDA complex (C_1) then receives a nucleophilic attack by the sulfur atom of PSAA incorporating PSAA into C_1 to form termolecular complex (C_2). The development of positive charge on the sulfur atom of PSAA in the intermediate complex (C_2) as a result of nucleophilic attack of PSAA is confirmed from the result of the reaction with different substituents in the phenyl ring of PSAA. The rate acceleration by electron-releasing substituents and retardation by electron-withdrawing groups in the *para*- and *meta*-positions can be explained on the basis of stabilization of the positive center on sulfur atom by electron-releasing substituents

and destabilization by electron-withdrawing substituents. The supporting evidence for the formation of termolecular complex (C_2) as a result of binding of PSAA with C_1 is obtained from the perceptible change in absorbance at 351 nm (Fig. 4c).

The kinetic evidence for the formation of C_2 is ascertained from the large negative value of entropy of activation observed in PDA catalyzed reaction (Table 2) as compared with the low value of entropy of activation obtained in the reaction without PDA [15] ($-24.5 \text{ KJ mol}^{-1}$). This may be taken as an evidence for the association of PDA moiety in the transition state leading to the formation of more orderly rigid transition state. The linear plot between k_1^{-1} and $[PSAA]^{-1}$ with definite intercept and non-integral kinetic order with respect to PSAA indicate that the ternary complex, $[Cr(VI)\text{-PSAA-PDA}]$ is formed in an equilibrium step (eq.6). The Michaelis-Menten constant, K_m computed for the binding of PSAA with C_1 also shows that the binding of PSAA with the active oxidizing species is moderately high. The complex C_2 then experiences a redox decomposition slowly in the rate-determining step giving rise to the products Cr(IV)-PDA, CO_2 and methylphenyl sulfone (Scheme 2, eq.7).



(C_1)

Scheme 1. Formation of active oxidizing species

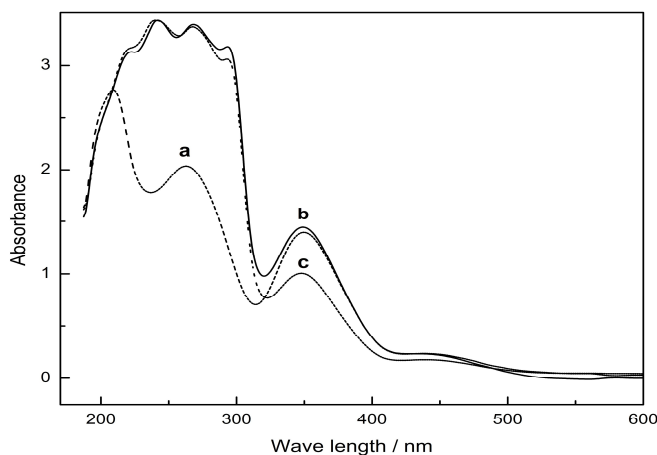
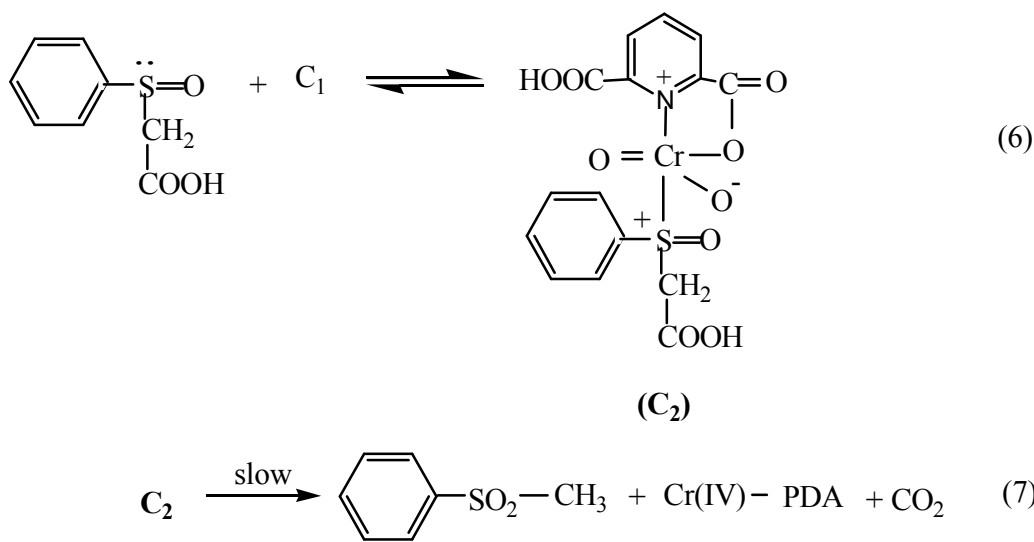


Fig. 4. UV-vis absorption spectra of Cr(VI) with PDA (a) Cr(VI); (b) Cr(VI)-PDA; (c) Cr(VI)-PDA-PSAA

$[Cr(VI)] = 5.0 \times 10^{-4} \text{ mol dm}^{-3}$; $[PSAA] = 5.0 \times 10^{-2} \text{ mol dm}^{-3}$; $[PDA] = 5 \times 10^{-2} \text{ mol dm}^{-3}$.



Scheme 2. Mechanism of PDA catalyzed redox reaction of PSAA and Cr(VI)

The Cr(IV)-PDA species formed in the reaction as a result of two-electron transfer participates in the faster steps [32] with Cr(VI)-PDA to give Cr(V)-PDA and consequently Cr(V)-PDA oxidizes another PSAA molecule and itself gets reduced to Cr(III)-PDA species. The Cr(V)-Cr(III) couple has a potential of 1.75 V which would enable the rapid conversion of Cr(V) to Cr(III) after the reaction with the substrate [33-35].

4. CONCLUSION

The PDA catalyzed redox reaction of phenylsulfonyl acetic acid and Cr(VI) follows Michaelis-Menten kinetics with respect to PSAA as well as PDA. A mechanism involving reversible formation of a ternary complex, Cr(VI)-PDA-PSAA followed by a redox decomposition in the rate-determining step giving rise to the products Cr(IV)-PDA, CO₂ and methylphenyl sulfone is proposed. The substituent effect and linear free energy relationship are also discussed.

COMPETING INTERESTS

Authors have declared that no competing interests exist.

REFERENCES

- Nathan LC, Mai TD. Influence of the spectator cation on the structure of anionic pyridine-2,6-dicarboxylate complexes of

- cobalt(II), nickel(II), and copper(II). *J Chem Cryst.* 2000;30:509-518.
- Aghabozorg H, Bahrami Z, Tabatabaie M, Ghadermazi M, Attar Gharamaleki J. Poly[propane-1,3-diammonium [diaqua-tetrakis (μ₄-benzene-1,2,4,5-tetracarboxylato) nickelate(II)] hemihydrate]. *Acta Cryst.* 2007;63:2022-2023.
- Aghajani Z, Sharif MA, Aghabozorg H, Naderpour A. Bis(2,4,6-triamino-1,3,5-triazin-1-ium) bis(pyridine-2,6-dicarboxylato)zincate(II) decahydrate. *Acta Cryst.* 2006;62:830-832.
- Sharif MA, Aghabozorg H, Shokrollahi A, Kickelbick G, Moghimi A, Shamsipur M. Novel proton transfer compounds containing 2,6-pyridinedicarboxylic acid and melamine and their Pb^{II} complex: Synthesis, characterization, crystal structure and solution studies. *Polish J Chem.* 2006;80:847-863.
- Crans DC. Chemistry and insulin-like properties of vanadium(IV) and vanadium(V) compounds. *J Inorg Biochem.* 2000;80:123-131.
- Yang L, Crans DC, Miller SM, la Cour A, Anderson OP, Kaszynski PM, Godzala ME, Austin LD, Willsky GR. Cobalt(II) and cobalt(III) dipicolinate complexes: Solid state, solution, and in vivo insulin-like properties. *Inorg Chem.* 2002;41:4859.
- Iwahashi H, Kawamori H, Fukushima K. Quinolinic acid, α-picolinic acid, fusaric acid, and 2,6-pyridinedicarboxylic acid enhance the Fenton reaction in phosphate

- buffer Chem-Bio Interact. 1999;118:201-215.
8. Chauhan Jayprakash S, Pandya Ajit V. Spectrophotometric determination of Mn (II) ion by Pyridine 2, 6 dicarboxylic acid. Int J Eng Sci Invent. 2013;2:36-43.
 9. Gok E, Ates S. Fluorimetric detection of insulin in the presence of Eu(III)-{pyridine-2,6-dicarboxylate} tris complex. Turk J Chem. 2001;25:81-91.
 10. Muller G, Schmidt B, Jiricek J, Hopfgartner G, Riehl JP, Buenzli JCG. Lanthanide triple helical complexes with a chiral ligand derived from 2,6-pyridinedicarboxylic acid. J Chem Soc Dalton Trans. 2001;18:2655-2662.
 11. Yin XH, Tan MY. Synthesis of Novel Multifunctional Pyridine-2,6-Dicarboxylic Acid Derivatives. Synth Commun. 2003;33:1113-1120.
 12. Tang R, Zhao Q, Yan Z, Luo Y. Synthesis of Novel Derivatives of Pyridine-2,6-dicarboxylic Acid. Synth Commun. 2006;36:2027-2034.
 13. Liang X, Weishaupl M, Parkinsom JA, Parsons S, McGregor PA, Sadler PJ. Selective Recognition of Configurational Substates of Zinc Cyclam by Carboxylates: Implications for the Design and Mechanism of Action of Anti-HIV Agents. Chem Eur J. 2003;9:4709-4717.
 14. Subramaniam P, Thamil Selvi N. Spectral evidence for the one-step three-electron oxidation of phenylsulfinyl acetic acid and oxalic acid by Cr(VI). Am J Anal Chem. 2013;4:20-29.
 15. Subramaniam P, Thamil Selvi N, Sugirtha Devi S. Spectral and mechanistic investigation of oxidative decarboxylation of phenylsulfinyl acetic acid by Cr(VI). J Korean Chem Soc. 2014;58:17-24.
 16. Subramaniam P, Sugirtha Devi S, Anbarasan S. Proximal effect of the nitrogen bases in the oxidative decarboxylation of phenylsulfinyl acetic acids by oxo(salen)chromium(V) complexes. J Mol Catal A Chem. 2014;390:159.
 17. Subramaniam P, Thamil Selvi N. Micellar and Substituent Effects on the Redox reaction of Phenylsulfinyl acetic Acid and Cr(VI). Int J Adv Sci Tech Res. 2014;4:418-427.
 18. Walker D, Leib J. The Acid-Catalysed Cleavage of Phenylsulfinyl acetic Acid. Can J Chem. 1962;40:1242-1248.
 19. Kenney WJ, Walsh JA, Davenport DA. An Acid-Catalyzed Cleavage of Sulfoxides. J Am Chem Soc. 1961;83:4019-4022.
 20. Perrin DD, Armargo ALF, Perrin DK. Purification of Laboratory Chemical, 2nd Ed.; Pergaman, New York, 1980.
 21. Pouchart CJ. The Aldrich Library of IR Spectra, 3rd Ed.; Aldrich Chemical Co.: Milwaukee, WI; 1981.
 22. Figgis BN. Introduction to Ligand Fields. Wiley Eastern Limited: New Delhi, India. 1966;222.
 23. Jorgensen CK. Absorption Spectra and Chemical Bonding in Complexes. Pergamon Press Ltd.: Oxford/London, 1964, p. 290.
 24. Abid M, Khan Z. The effect of complexing agents on the DMF-chromium(VI) reaction. A kinetic study. Transition Met Chem. 2003;28:79-84.
 25. Khan Z, Kabir-ud-Din. Kinetics and Mechanism of ethylenediaminetetracetic acid, 2,2' bipyridyl, and 1,10 phenanthroline assisted Cr(VI) oxidation of 2-propanol. Transition Met Chem. 2002;27:832-839.
 26. Islam M, Saha B, Das AK. Kinetics and mechanism of picolinic acid promoted chromic acid oxidation of maleic acid in aqueous micellar media. J Mol Catal A Chem. 2007;266:21-30.
 27. Bayen R, Das AK. Kinetics and Mechanism of Oxidation of D-Galactose by Chromium(VI) in Presence of 2,2'-Bipyridine Catalyst in Aqueous Micellar Media. The Open Catalysis Journal. 2009;2:71-78.
 28. Sathyanarayanan K, Pavithra C, Lee CW. Kinetics and Mechanism of EDTA-Catalyzed Oxidation of (S)-Phenylmercaptoacetic Acid by Chromium(VI). J Ind Eng Chem. 2006;12:727-732.
 29. Das AK, Mondal SK, Kar D, Das M. Micellar effect on the reaction of picolinic acid catalyzed chromium(VI) oxidation of dimethyl sulfoxide in aqueous acidic media: A kinetic study. Int J Chem Kinet. 2001;33:173-181.
 30. Bayen R, Islam M, Das AK. Micellar effect on the reaction of chromium(VI) oxidation of some representative α -hydroxy acids in the presence and absence of 2,2'-bipyridyl in aqueous acid media: A kinetic study. Indian J Chem. 2009;48:1055-1061.

31. Das AK. Micellar effect on the kinetics and mechanism of Cr(VI) oxidation of organic substrates. *Coord Chem Rev.* 2004;248:81-99.
32. Cooper N, Staudt GE, Smalser ML, Setz LM, Haight GP. Ligand capture in reductions of chromium(VI). *Inorg Chem.* 1973;12:2075-2079.
33. Westheimer FH. The Mechanisms of Chromic Acid Oxidations. *Chem Rev.* 1949;45:419-451.
34. Watanabe W, Westheimer FH. The Kinetics of the Chromic Acid Oxidation of Isopropyl Alcohol: The Induced Oxidation of Manganous Ion. *Chem Phys.* 1949;17:61.
35. Perez-Benito J F, Arias C, Lamrhari D. Evidence for the involvement of chromium(II) as an intermediate in the reduction of chromium(VI) to chromium(III) by formaldehyde. *J Chem Soc Chem Commun.* 1992;472-474.

© 2015 Subramaniam and Thamil Selvi; This is an Open Access article distributed under the terms of the Creative Commons Attribution License (<http://creativecommons.org/licenses/by/4.0>), which permits unrestricted use, distribution, and reproduction in any medium, provided the original work is properly cited.

Peer-review history:

The peer review history for this paper can be accessed here:
<http://www.sciencedomain.org/review-history.php?iid=900&id=16&aid=8182>